The Canadian Mineralogist
Vol. 51, pp. 243-251 (2013)
DOI: 10.3749/canmin.51.2.243

THE CRYSTAL STRUCTURE OF YOFORTIERITE

FRANK C. HAWTHORNE§ AND YASSIR A. ABDU

Department of Geological Sciences, University of Manitoba, Winnipeg, Manitoba R3T 2N2 Canada

KIMBERLY T. TAIT AND MALCOLM E. BACK

Department of Natural History, Mineralogy, Royal Ontario Museum, 100 Queen's Park, Toronto, Ontario M5S 2C6, Canada

ABSTRACT

The crystal structure of yofortierite, $(Mn^{2+},Mg,Fe^{3+},\square)_5Si_8O_{20}(OH,H_2O)_2(H_2O)_7$, monoclinic, *C*2/*m*, *Z* = 4, *a* 14.1686(12), *b* 17.8583(16), *c* 5.2919(5) Å, β 105.878(1)°, *V* 1287.9(3) Å^3, has been refined to R_1 = 4.9 % for 1795 unique ($F_o > 4\sigma F$) reflections collected on a Bruker D8 three-circle diffractometer equipped with a rotating-anode generator (Mo*K*α X-radiation), a multi-layer optics incident-beam path, and an APEX-II CCD detector. Chemical analysis by electron microprobe plus Fe^{3+} determination by Mössbauer spectroscopy gave SiO_2 51.78, Al_2O_3 0.05, TiO_2 0.15, Fe_2O_3 1.84, MnO 22.97, ZnO 0.99, MgO 4.32, CaO 1.10, H_2O_{calc} 16.69, sum 99.89 wt.%. The resulting empirical formula is $(Mn_{3.01}Mg_{1.00}Zn_{0.11}Ca_{0.18}Fe^{3+}_{0.21}Ti_{0.02}Al_{0.01}\square_{0.46})_{\Sigma=5}Si_{8.00}O_{20}[(OH)_{1.34}(H_2O)_{0.66}]_{\Sigma=2}(H_2O)_7$. Yofortierite is a palygorskyite-group mineral. There are two tetrahedrally coordinated *T* sites occupied by Si with <Si–O> distances of 1.621 and 1.617 Å, and three octahedrally coordinated *M* sites, occupied primarily by Mn^{2+} and Mg with minor Fe^{3+} and □, with <*M*–O> distances of 2.147, 2.079, and 2.183 Å. The <*M*–O> distances indicate strong order of M cations over the three *M* sites, with the smaller cations and vacancies ordered at the *M*(2) site and Ca ordered at the *M*(3) site. The presence of vacancies at the *M*(2) site locally couple with the replacement of $(OH)^-$ at the O(4) site by $(H_2O)^o$, giving rise to strong short-range order, and H_2O is incorporated into the framework part of the structure by the substitution $Mn^{2+} + (OH)^- = \square + (H_2O)^o$ which is coupled to the substitution $Mn^{2+} = Fe^{3+}$ by the requirement of electroneutrality.

Keywords: yofortierite, crystal structure, Mössbauer spectrum, electron microprobe analysis, short-range order

INTRODUCTION

Yofortierite was described as the Mn-analogue of palygorskite by Perrault *et al*. (1975), and the ideal formula of yofortierite is generally written as $Mn_5(Si_8O_{20})(OH)_2(H_2O)_9$ (Back & Mandarino 2008). The minerals of the palygorskite group show a range of chemical compositions and structural variations, but there is reasonable coherence between their chemical formulae, unit-cell dimensions, and space-group symmetry (Table 1). The structural unit common to these four minerals is an $[M_5(OH)_2(T_8O_{20})]$ framework, essentially amphibole I-beams that link by sharing tetrahedron corners to form a framework of tetrahedra and octahedra. Palygorskyite forms one end of the palesepiole polysomatic series (Ferraris & Gula 2005), the other end being sepiolite, and various members of this series are known, *e.g*., kalifertisite (Ferraris *et al*. 1998), together with related minerals, *e.g*., intersilite (Egorov-Tismenko *et al*. 1996, Yamnova *et al*. 1996) and raite (Pluth *et al*. 1997). The structures of the other members of the palygorskyite group have been reported (Table 1) and all have significant vacancies at the octahedrally coordinated *M* sites, suggesting that the formula $Mn_5(Si_8O_{20})(OH)_2(H_2O)_9$ generally given for yofortierite may be rather idealistic. Here we report a more accurate determination of the structure and chemical formula of yofortierite, and show that short-range order and local bond-valence requirements exert considerable control on the chemical composition of this mineral.

X-RAY DATA COLLECTION AND STRUCTURE SOLUTION-REFINEMENT

The material from which we selected the crystal is from the Poudrette Quarry, Mont St.-Hilaire, Rouville County, Québec, and is from the mineral collection of the Department of Natural History, Royal Ontario Museum, specimen number M34865. A single crystal of yofortierite (10 × 20 × 220 μm) was mounted on a Bruker D8 three-circle diffractometer equipped with a

§ *Email address*: frank_hawthorne@umanitoba.ca

rotating-anode generator (Mo$K\alpha$ X-radiation), a multilayer optics incident-beam path, and an APEX-II CCD detector. A sphere of X-ray diffraction data (20,344 reflections) was collected to 60° 2θ using 60 s per 0.3° frame with a crystal-to-detector distance of 5 cm. The unit-cell parameters were obtained by least-squares refinement of 9955 reflections ($I > 10\sigma I$), and are given in Table 2. Empirical absorption corrections (SADABS; Sheldrick 2008) were applied and identical data merged to give 7519 reflections covering the entire Ewald sphere and 1946 unique reflections with $R_{merge} = 1.5\%$.

As with tuperssuatsiaite (Cámara *et al*. 2002), there are numerous weak reflections violating the *C*-centering (using a test integration on a primitive cell). However, precession slices produced from the data frames reveal extremely poorly defined weak diffuse intensity in these regions that does not conform to sensible diffraction maxima that can be reliably indexed or integrated. In general, all diffraction spots on the *C*-centered cell have diffuse margins and show pronounced elongation along **a***. Structure refinement was initiated with the coordinates and site labeling for tuperssuatsiaite (Cámara *et al*. 2002), and converged to $R_1 = 4.9\%$ and $wR_2 = 13.9\%$. At the final stages of refinement, a peak was noted in the difference-Fourier map ~1 Å from the O(5) anion that the incident bond-valence (see later discussion) indicates is an (OH) group. Refinement of the positional coordinates of the H atom with fixed isotropic-displacement parameter and occupancy, and a soft constraint that O(donor)–H ≈ 0.98 Å, together with all other variable positional coordinates, anisotropic-displacement parameters, and site-scattering values (Hawthorne *et al*. 1995) for the *M* sites, converged at an R_1 index of 4.90%. Final atom coordinates, anisotropic-displacement parameters, selected interatomic distances and angles, and refined site-scattering values are given in Tables 3, 4, and 5. Bond valences were calculated with the curves of Brown & Altermatt (1985) and are given in Table 6.

Mössbauer Spectroscopy

Transmission Mössbauer-spectroscopy measurement was done at room temperature (RT) on a powdered sample using a ^{57}Co(Rh) source. Approximately 2 mg of sample was mixed with sugar and finely ground under acetone to avoid oxidation. The mixture was then loaded into a Pb ring (2 mm inner diameter) and covered by tape on both sides. The resultant Mössbauer absorber contains ~1 mg Fe/cm^2. The spectra were analyzed using a Voigt-based quadrupole-splitting-distribution (QSD) method (Rancourt & Ping 1991). The Mössbauer

TABLE 1. MINERALS OF THE PALYGORSKYITE GROUP

Name	Formula	*a* (Å)	*b* (Å)	*c* (Å)	β (°)	Space group	Ref.
palygorskite	$(Mg,Al)_4[Si_8O_{20}](OH)_2(H_2O)_8$	12.7–13.2	17.8–18.1	5.12–5.24	91–107	*C*2/*m*	(1)
tuperssuatsiaite	$Na_{(2-x)}(Fe^{3+},Mn)_3[Si_8O_{20}](OH)_2(H_2O)_4$	14.034(7)	17.841(7)	5.265(2)	103.67(4)	*C*2/*m*	(2)
yofortierite*	$(Mn^{2+},Mg,Fe^{3+},\square)_5[Si_8O_{20}](OH)_2(H_2O)_9$	14.169(1)	17.858(2)	5.2919(5)	105.878(1)	*C*2/*m*	(3)
windhoekite	$Ca_2Fe^{3+}{}_{(3-x)}[(Si,Al)_8O_{20}](OH)_4\ (H_2O)_{10}$	14.319(5)	17.825(4)	5.242(1)	103.5(2)	*C*2/*m*	(4)

* The currently accepted formula of yofortierite is given; the present study modifies this slightly.
References: (1) Chisholm (1992), Artioli & Galli (1994), Chiari *et al.* (2003), Giustetto & Chiari (2004), Post & Heaney (2008); (2) Karup-Møller *et al.* (1984), von Knorring *et al.* (1992), Cámara *et al.* (2002); (3) Perrault *et al.* (1975), this study; (4) Chukanov *et al.* (2012).

TABLE 2. MISCELLANEOUS INFORMATION FOR YOFORTIERITE

a (Å)	14.1686(12)	crystal size (μm)	10 × 20 × 220
b	17.8583(16)	Radiation	Mo$K\alpha$
c	5.2919(5)	No. of reflections	20344
β (°)	105.878(1)	No. unique reflections	1946
V (Å^3)	1287.9(3)	No. $\lvert F_o\rvert > 4\sigma\lvert F\rvert$	1795
Sp. Gr.	*C*2/*m*	R_{merge} %	1.47
Z	4	R_1 %	4.90
		wR_2 %	13.8
		GooF	1.398

Cell content 4 $[(Mn,Mg,Fe^{3+},\square)_5Si_8O_{20}(OH)_2(H_2O)_9]$
$R_1 = \Sigma(|F_o| - |F_c|) / \Sigma|F_o|$
$wR_2 = [\Sigma w (F_o^2 - F_c^2)^2 / \Sigma w (F_o^2)^2]^{½}$, w = 1 / $[\sigma^2(F^2) + (0.0441*P)^2 + 8.30*P]$
where P = $(Max(F_o^2,0) + 2*F_c^2) / 3$

TABLE 3. ATOM COORDINATES AND ANISOTROPIC-DISPLACEMENT PARAMETERS FOR YOFORTIERITE

Atom	*x*	*y*	*z*	U_{11}	U_{22}	U_{33}	U_{23}	U_{13}	U_{12}	U_{eq}
Si(1)	0.29667(7)	0.41441(5)	0.02119(18)	0.0204(5)	0.0104(4)	0.0120(4)	–0.0003(3)	0.0064(3)	–0.0012(3)	0.0139(2)
Si(2)	0.29544(7)	0.33245(5)	0.52172(18)	0.0233(5)	0.0110(4)	0.0112(4)	–0.0010(3)	0.0056(3)	–0.0015(3)	0.0150(2)
Mn(1)	½	½	0	0.0209(7)	0.0132(6)	0.0108(6)	0	0.0059(5)	0	0.0147(4)
Mn(2)	½	0.41128(5)	½	0.0194(5)	0.0208(5)	0.0115(4)	0	0.0051(3)	0	0.0171(3)
Mn(3)	½	0.31362(5)	0	0.0229(5)	0.0192(5)	0.0124(4)	0	0.0040(3)	0	0.0183(3)
O(1)	0.41446(19)	0.40991(14)	0.1074(5)	0.0211(12)	0.0160(11)	0.0171(12)	–0.0020(9)	0.0070(10)	–0.0013(9)	0.0177(5)
O(2)	0.4124(2)	0.33161(17)	0.6084(5)	0.0258(14)	0.0303(14)	0.0155(12)	–0.0031(10)	0.0058(10)	0.0051(11)	0.0238(6)
O(3)	¼	¼	½	0.058(3)	0.0134(17)	0.025(2)	–0.0017(14)	0.0132(19)	–0.0124(18)	0.0316(10)
O(4)	0.5754(3)	½	0.3966(7)	0.0252(19)	0.0191(17)	0.0189(17)	0	0.0075(15)	0	0.0208(7)
O(5)	0.2572(3)	½	0.0070(8)	0.0272(19)	0.0131(15)	0.0236(18)	0	0.0076(15)	0	0.0212(7)
O(6)	0.25093(19)	0.37121(14)	0.2329(5)	0.0242(13)	0.0183(12)	0.0155(11)	0.0047(9)	0.0074(9)	–0.0003(10)	0.0190(5)
O(7)	0.2514(2)	0.37756(15)	0.7334(5)	0.0263(13)	0.0201(12)	0.0141(11)	–0.0053(9)	0.0066(10)	–0.0021(10)	0.0200(5)
O(8)	0.4065(3)	0.2306(3)	0.1033(8)	0.052(2)	0.052(2)	0.047(2)	0.0045(18)	0.0121(18)	–0.0185(19)	0.0506(10)
O(9)	0.5776(12)	0	0.276(4)	0.128(12)	0.145(14)	0.25(2)	0	0.122(14)	0	0.160(9)
O(10)	½	0.1261(6)	½	0.089(7)	0.074(6)	0.085(7)	0	–0.003(5)	0	0.088(4)
H	0.6472(4)	½	0.456(19)							0.07(3)

TABLE 4. SELECTED INTERATOMIC DISTANCES (Å) AND ANGLES (°) IN YOFORTIERITE

Si(1)–O(1)	1.607(3)	*Si*(2)–O(2)	1.594(4)
Si(1)–O(5)	1.622(3)	*Si*(2)–O(3)	1.599(1)
Si(1)–O(6)	1.633(2)	*Si*(2)–O(6)	1.639(3)
Si(1)–O(7)a	1.621(3)	*Si*(2)–O(7)	1.636(3)
<*Si*(1)–O>	1.621	<*Si*(2)–O>	1.617
M(1)–O(1) x4	2.181(3)	*M*(3)–O(1) x2	2.264(3)
M(1)–O(4) x2	2.078(4)	*M*(3)–O(2)a x2	2.129(3)
<*M*(1)–O>	2.147	*M*(3)–O(8) x2	2.155(4)
		<*M*(3)–O>	2.183(4)
M(2)–O(1) x2	2.100(3)		
M(2)–O(2) x2	2.070(3)	O(4)–H	0.98
M(2)–O(4) x2	2.067(3)	H–O(5)	2.791
<*M*(2)–O>	2.079	O(4)–H–O(5)	120

a: *x*, *y*, *z*–1.

TABLE 5. REFINED SITE-SCATTERING VALUES AND ASSIGNED SITE-POPULATIONS FOR YOFORTIERITE

Site	Site scattering (*epfu*)		Site population (*apfu*)
	Refined	Normalized	
T(1)	56	–	Si
T(2)	56	–	Si
M(1)	19.9(2)	19.4	0.57 Mn + 0.43 Mg
M(2)	42.7(2)	41.7	0.01 Al + 0.02 Ti^{4+} + 0.22 Fe^{3+} + 1.27 Mn^{2+} + 0.11 Zn + 0.34 □ + 0.03 Mg
M(3)	42.9(2)	41.8	0.18 Ca + 1.26 Mn + 0.56 Mg
O(4)	–	–	1.34 OH + 0.66 H_2O

TABLE 6. BOND VALENCES (*vu*) FOR YOFORTIERITE

	T(1)	*T*(2)	*M*(1)	*M*(2)	*M*(3)	H	Sum
O(1)	1.047		$0.314^{x4\downarrow}$	$0.350^{x2\downarrow}$	$0.278^{x2\downarrow}$		1.989
O(2)		1.084		$0.380^{x2\downarrow}$	$0.400^{x2\downarrow}$		1.864
O(3)		$1.070^{x2\rightarrow}$					2.140
O(4)			$0.414^{x2\downarrow}$	$0.383^{x2\rightarrow\downarrow}$		0.90	2.080
O(5)	$1.005^{x2\rightarrow}$					0.10	2.110
O(6)	0.976	0.960					1.936
O(7)	1.008	0.968					1.976
O(8)					$0.373^{x2\downarrow}$		0.373
O(9)							–
O(10)							–
Sum	4.036	4.082	2.084	2.226	2.102	1.00	

TABLE 7. MÖSSBAUER PARAMETERS FOR YOFORTIERITE

Fe site	CS (mm/s)	QS (mm/s)	Rel. area (%)
Fe^{3+} (I)	0.35	0.50	56(4)
Fe^{3+} (II)	0.40	1.15	32(4)
Fe^{3+} (III)	0.46	2.11	12(4)

parameters are given in Table 7; the center shift (CS) is given relative to α-Fe at room temperature, and indicates that all Fe is in the trivalent state (Fig. 1).

Chemical Composition

Yofortierite (not the X-ray crystal) was analyzed with a JEOL JXA-8230 electron microprobe operating in wavelength-dispersion mode with an accelerating voltage of 10 kV, a specimen current of 10 nA, and a beam diameter of 5 μm. The following standards were used: adularia (Al, K); diopside (Si, Ca); rutile (Ti); chromite (Cr); gahnite (Zn); synthetic fayalite (Fe); synthetic hausmannite (Mn); synthetic forsterite (Mg); albite (Na); synthetic fluorphlogopite (F); scapolite (Cl). Ten points were analyzed, the data were reduced and corrected by the Armstrong *phi(rho-z)* correction as contained in CITZAF; very minor F and Cl were detected, but analysis of the epoxy indicates that this is probable epoxy contamination. Mössbauer spectroscopy showed that all Fe is in the trivalent state. The mean chemical composition is given in Table 8.

TABLE 8. CHEMICAL COMPOSITION (wt.%) AND UNIT FORMULA (*apfu*) FOR YOFORTIERITE

SiO_2	51.78(11)	Si	8.00
Al_2O_3	0.05(2)		
TiO_2	0.15(5)	Al	0.01
Fe_2O_3*	1.84(18)	Ti	0.02
MnO	22.97(77)	Fe^{3+}	0.21
ZnO	0.99(7)	Mn	3.01
MgO	4.32(23)	Zn	0.11
CaO	1.10(6)	Mg	1.00
H_2O**	16.69	Ca	0.18
Sum	99.89	Sum	4.54
		(OH)	1.34
		H_2O	0.66
		H_2O	7.27

*Oxidation state determined by Mössbauer spectroscopy
**H_2O calculated as discussed in the text.

Calculation of the Chemical Formula

Initial normalization of the chemical formula on 22 (O + OH) *pfu* (per formula unit) gave Si considerably in excess of 8 atoms *pfu* (~8.2 *apfu*). Re-analysis with a different electron microprobe confirmed the original values, and suggested that the normalization procedure used for calculating the formula was not appropriate. The presence of significant vacancies at the *M* sites (Tables 5 and 8) raises the issue of electroneutrality: the ideal formula $Mn_5Si_8O_{20}(OH)_2(H_2O)_9$ is neutral, but this situation is perturbed by the occurrence of significant vacancies at the *M* sites (*i.e.*, substituting for Mn^{2+}). To some extent, this is compensated by the occurrence of Fe^{3+} (and very minor Al and Ti) at the *M* sites, but there are insufficient higher-valence cations to produce electroneutrality, and some other mechanism must also be operative. The only possibility is to reduce the amount of negative charge in the structure. This is most easily done by substituting (H_2O) for (OH); the amount of (H_2O) so introduced may be calculated as follows: (1) The charge of the cations at the *M* sites was calculated, and the deficiency from the ideal value of 10^+ was compensated by introducing an equivalent amount of (H_2O) substituting for (OH) at the O(4) site.

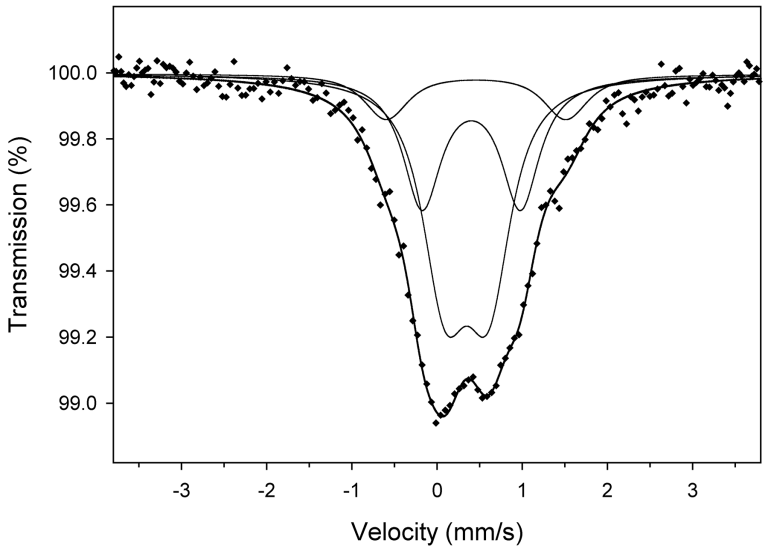

FIG. 1. The Mössbauer spectrum of yofortierite consisting of three Fe^{3+} doublets.

This amount of (H_2O) was fed back into the calculation of the formula and the amount of (OH) was adjusted accordingly, producing a minor change in cation stoichiometry. This process was repeated to self-consistency.

A separate issue involves the amount of (H_2O) occurring in the channels of the structure [*i.e.*, at the O(9) and O(10) sites]. If these sites are fully occupied by (H_2O), they will contribute $(H_2O)_8$ to the formula unit. However, site-scattering refinement (Table 5) indicates that these two sites are not fully occupied. Confidence in this result is not strong: the resultant site-populations are 3.60(13) and 3.67(10) (H_2O) groups *pfu*, but they do suggest that the (H_2O) content is somewhat deficient relative to the ideal value. Thus we used the value of 7.27 (H_2O) groups *pfu* in the calculation of the chemical formula. The value used for the (H_2O) groups in the channels does not affect the stoichiometry of the rest of the constituents in the formula; it only effects the sum of the oxides in the chemical composition.

The final chemical composition is given in Table 8. The empirical formula is $Ca_{0.18}Mn^{2+}_{3.01}Mg_{1.00}Zn_{0.11}Fe^{3+}_{0.21}Ti_{0.02}Al_{0.01}Si_{8.00}O_{20}(OH)_{1.34}(H_2O)_{7.93}$, the idealized formula is $(Mn^{2+},Mg,Fe^{3+},\square)_5Si_{80}O_{20}(OH,H_2O)_2(H_2O)_7$ and the endmember formula is $Mn^{2+}_5Si_8O_{20}(OH)_2(H_2O)_8$. It is interesting to note that the "excess Si" observed in the initial calculation has disappeared; this "excess Si" was the result of ignoring the substitution of (H_2O) for (OH) in the formula of yofortierite.

DESCRIPTION OF THE STRUCTURE

Cation sites: coordination and occupancy

There are two sites, labeled *T*(1) and *T*(2), that are tetrahedrally coordinated by O anions with <*T*–O> distances of 1.621 and 1.617 Å, respectively, and these bond lengths and the site scattering are compatible with occupancy of these sites by Si. There are three *M* sites, *M*(1), *M*(2) and *M*(3), that the formula and refined site-scattering values (Hawthorne *et al*. 1996) indicate to be occupied by Mn and Mg, with minor Fe, Ca, Zn, Na, Ti, and Al. Site-scattering refinement can resolve site occupancy for only two scattering species (Hawthorne 1983), and hence mean bond lengths and ionic radii (Shannon 1976) are also used to indicate site-occupancies. The sum of the refined *M*-site-scattering values (Table 5) is 105.5 *epfu*, whereas the effective scattering from the sum of the *M* site-populations (Table 8) is 100.2 *epfu*. The assigned site populations should fit these two values equally well, and this may be done by adjusting the site-scattering values and the contents of the three *M* sites such that their sums are equal to the average value of the sum of the refined *M*-site-scattering values and the effective scattering from the sum of the *M* site-populations: 102.9 *epfu*. We may make what could be called an "educated" crystal-chemical assignment in the following way. Let us assume that the vacancies are ordered at the *M*(2) site, together with the small higher valence cations Fe^{3+} and Ti^{4+}. This is not a bad starting assumption, as the remaining *M*-site cations are Mn^{2+} and Mg, with radii of 0.83 and 0.72

Å, respectively, and the aggregate radius of the *M*(2) cations must be approximately 2.079 – 1.360 = 0.719 Å, *i.e.*, *M*(2) cannot be occupied solely by Mn and Mg because the mean bond length is too short. Moreover, <*M*(3)–O> is much larger than <*M*(1)–O> (2.183 *versus* 2.147 Å), suggesting that Ca, by far the largest *M* cation, is ordered at *M*(3). With these assumptions, we may calculate the possible site-populations for *M*(1) and *M*(3) from the refined site-scattering values (Table 5): 25 x $Mn^{M(1)}$ + 12 x (1 – $Mn^{M(1)}$) = 19.4, whence *M*(1) = 0.57 Mn + 0.43 Mg; and 0.18 Ca + 25 x $Mn^{M(3)}$ + 12 x (2 – $Mn^{M(3)}$) = 41.8, whence *M*(3) = 0.18 Ca + 1.25 Mn + 0.57 Mg. Subtraction of the *M*(1) and *M*(3) constituents from the normalized *M*-site composition from the electron-microprobe analysis gives the following: *M*(2) = 0.01 Al + 0.02 Ti^{4+} + 0.22 Fe^{3+} + 1.27 Mn^{2+} + 0.11 Zn + 0.03 Mg + 0.34 □.

Anion sites

The bond valences given in Table 6 indicate that the O(1), O(2), O(3), O(5), O(6), and O(7) anions are O^{2-}, and correspond to the O_{20} part of the chemical formula. The O(4) anion is bonded to three *M* cations, resulting in an incident bond-valence at O(4) of ~1.2 *vu*, ignoring the presence of vacancies at the *M* sites. Hence the O(4) site is occupied predominantly by a monovalent anion, and corresponds to the $(OH)_2$ part of the chemical formula. The O(8) anion is adjacent to only one M(3) site (Table 6). The maximum bond-valence incident at O(8) is << 1.0 *apfu*, and hence O(8) is fully occupied by (H_2O). The O(9) and O(10) sites are not bonded to any cations and hence must be occupied by (H_2O). Assuming full occupancy of the O(8), O(9), and O(10) sites, they provide 8 (H_2O) groups *pfu*, one less (H_2O) group than required by the ideal formula: $Mn_5Si_8O_{20}(OH)_2(H_2O)_9$. Moreover, the equivalent isotropic-displacement factor for the O(9) and O(10) sites are very high (Table 3) compared with the other anions in the formula, indicating either considerable positional disorder or partial occupancy (or both).

Structural connectivity

The *T*(1) and *T*(2) tetrahedra link by sharing corners to form a [T_8O_{22}] ribbon that is identical to the ribbon in amphiboles (Hawthorne & Oberti 2007). The *M*(1), *M*(2), and *M*(3) octahedra link by sharing edges to form a ribbon of octahedra identical to the *M*(1,2,3) ribbon in amphiboles. Both of these structural elements extend in the **c** direction and define the repeat distance of ~5.3 Å in this direction (Fig. 2). The apical vertices of the tetrahedra link to shared anions on each side of the ribbon of octahedra (Fig. 2) to form an I-beam (Fig. 3). These I-beams link in the **b**-direction through sharing anions between tetrahedra, forming large tunnels that are occu-

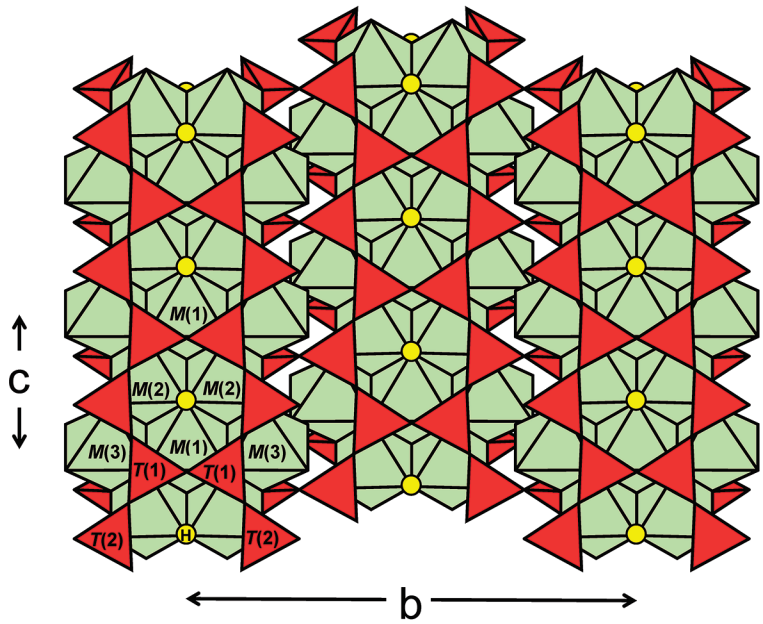

FIG. 2. The crystal structure of yofortierite projected onto (100); *T* tetrahedra are shown in red, *M* octahedra are shown in green, the H atom attached to the O(4) site [a mixture of (OH) and (H_2O)] is shown as a yellow circle.

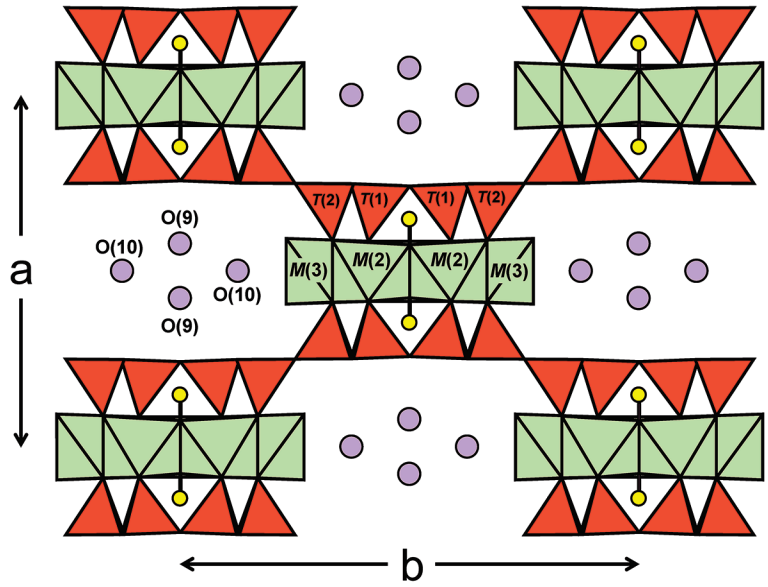

FIG. 3. The crystal structure of yofortierite projected onto (001). Legend as in Figure 2; the O(4)–H bond is shown as a thick black line, and (H_2O) groups at O(9) and O(10) are show as mauve circles.

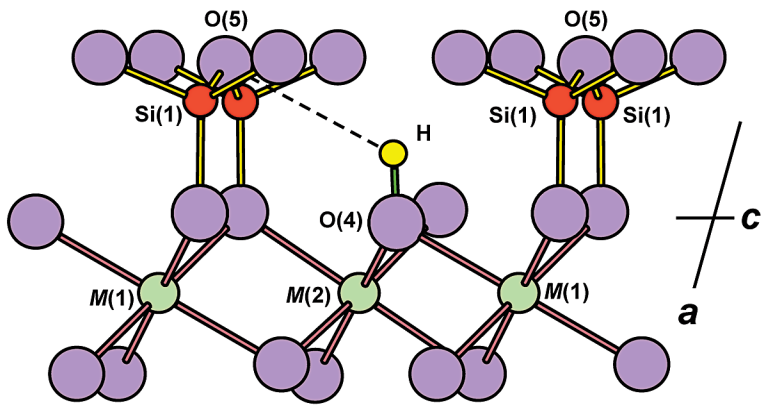

FIG. 4. The crystal structure of yofortierite projected onto (010); Si atoms are shown as red circles, M cations are shown as green circles, the H atom attached to the O(4) site [a mixture of (OH) and (H_2O)] is shown as a yellow circle, and the hydrogen bond from H to O(5) is shown by the dashed line.

pied by (H_2O) groups [O(9) and O(10) in Fig. 3]. The H atom located in this work forms an (OH) group with the O(4) atom as the donor anion. The O_{donor}–H bond projects orthogonal to the ribbon of octahedra and forms a hydrogen bond with the O(5) anion of the ribbon of tetrahedra (Fig. 4).

Short-range order

Crystal-structure refinement provides us with a long-range (average) image of the arrangement of atoms in a crystal, and bond-valence theory (Brown 2002) is commonly used with this average structure.

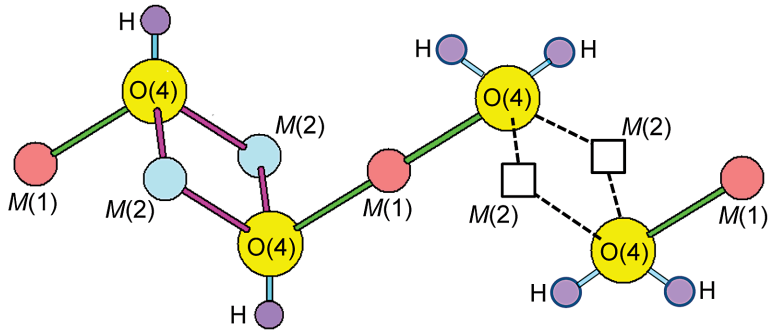

FIG. 5. Depiction of the short-range arrangements around the *M*(2) and O(4) sites; on the left, the *M*(2) sites are occupied by cations and the O(4) sites are occupied by $(OH)^-$ groups; on the right, the *M*(2) sites are occupied by vacancies and the O(4) sites are occupied by $(H_2O)^o$ groups; note that these two local arrangements can occur adjacent to each other without any steric problems.

However, Hawthorne *et al*. (1996) and Hawthorne (1997) showed that bond-valence theory can also be used on the local structure in a crystal to examine short-range arrangements in that crystal, and this approach has since been used extensively to examine short-range arrangements in minerals (Hawthorne & Della Ventura 2007, Hawthorne *et al*. 2005, 2006). A key aspect of the crystal chemistry of yofortierite is the presence of vacancies at the *M*(2) site (Table 5). Inspection of Table 6 shows that the O(4) anion is coordinated by one *M*(1) site and two *M*(2) sites. Where all *M* sites are locally occupied, the bond valence incident at O(4) accords with the valence-sum rule if O(4) is a donor anion to a hydrogen atom. However, the site populations (Table 5) indicate that *M*(2) has significant vacancy content which will have a major effect on the local bond-valence incident at O(4). In particular, if both *M*(2) sites locally associated with a specific O(4) O-atom are vacant, the bond valence incident at O(4) is ~0.40 *vu* and O(4) must be locally occupied by an (H_2O) group. The situation around O(4) is illustrated in Figure 5, which shows the coordination of a series of locally associated O(4) anions. As noted above, where two locally associated *M*(2) sites are occupied, the two locally associated O(4) anions are occupied by (OH) groups. Where two locally associated *M*(2) sites are vacant, the two locally associated O(4) anions are occupied by (H_2O) groups. Thus, because of the local configuration whereby two *M*(2) sites are adjacent to two O(4) sites, there is a 1:1 relation between the vacancy content at the *M* sites and the (H_2O) content of the O(4) site. However, because the relation $^{M(2)}M^{2+} + {}^{O(4)}(OH)^- \leftrightarrow {}^{M(2)}\square + {}^{O(4)}(H_2O)$ is not charge neutral, it must be accompanied by an additional substitution that acts such as to maintain overall electroneutrality: $M^{2+} \leftrightarrow M^{3+}$, as is the case here (Table 8), where Fe^{3+} (and minor Ti^{4+}) substitute for Mn^{2+}. Thus the principal substitutions affecting the composition of yofortierite are as follows:

$$Mn^{2+} + (OH)^- = \square + (H_2O)$$

and

$$Mn^{2+} = Fe^{3+}.$$

ACKNOWLEDGEMENTS

We thank Andreas Ertl and Tony Kampf for their comments on this paper, Mark Cooper for his help with collection of the X-ray data, and Tony Steede for SEM work. This work was supported by a Canada Research Chair in Crystallography and Mineralogy, by Natural Sciences and Engineering Research Council (NSERC) of Canada Discovery, Equipment and Major Installation grants, and by Innovation grants from the Canada Foundation for Innovation to FCH, and by an NSERC Discovery Grant to KTT.

REFERENCES

ARTIOLI, G. & GALLI, E. (1994) The crystal structures of orthorhombic and monoclinic palygorskite. *Materials Science Forum* **166–169**, 647–652.

BACK, M.E. & MANDARINO, J.A. (2008) *Fleischer's Glossary of Mineral Species*. Mineralogical Record Inc., Tucson, AZ.

BROWN, I.D. (2002) The chemical bond in inorganic chemistry. The bond valence model. Oxford University Press.

BROWN, I.D. & ALTERMATT, D. (1985) Bond-valence parameters obtained from a systematic analysis of the inorganic

crystal structure database. *Acta Crystallographica* **B41**, 244–247.

Cámara, F., Garvie, L.A.J., Devouard, B., Groy, T.L., & Buseck, P.R. (2002) The structure of Mn-rich tuperssuatsiaite: a palygorskite-related mineral. *American Mineralogist* **87**, 1458–1463.

Chiari, G., Giustetto, R., & Ricchiardi, G. (2003) Crystal structure refinements of palygorskite and Maya Blue from molecular, modeling and powder synchrotron diffraction. *European Journal of Mineralogy* **15**, 21–33.

Chisholm, J.E. (1992) Powder-diffraction patterns and structural models for palygorskite. *Canadian Mineralogist* **30**, 61–73.

Chukanov, N.V., Britvin, S.N., Blass, G., Belakovskiy, D.I., & Van, K.V. (2012) Windhoekite, $Ca_2Fe^{3+}_{3-x}(Si_8O_{20})(OH)_4{\cdot}10H_2O$, a new palygorskite-group mineral from the Aris phonolite, Namibia. *European Journal of Mineralogy* **24**, 171–179.

Egorov-Tismenko, Yu.K., Yamnova, N.A., & Khomyakov, A.P. (1996) A new representative of a series of chain-sheet silicates with inverted tetrahedral fragments. *Crystallography Reviews* **41**, 784–788.

Ferraris, G. & Gula, A. (2005) Polysomatic aspects of microporous minerals – heterophyllosilicates, palysepioles and rhodesite related structures. *Reviews in Mineralogy and Geochemistry* **57**, 69–104.

Ferraris, G., Khomyakov, A.P., Belluso, E., & Soboleva, S.V. (1998) Kalifersite, a new alkaline silicate from Kola Peninsula (Russia), based on a palygorskite-sepiolite polysomatic series, Locality: Kola Peninsula, Russia. *European Journal of Mineralogy* **10**, 865–874.

Giustetto, R. & Chiari, G. (2004) Crystal structure refinement of palygorskite from neutron powder diffraction. *European Journal of Mineralogy* **16**, 521–532.

Hawthorne, F.C. (1983) Quantitative characterization of siteoccupancies in minerals. *American Mineralogist* **68**, 287–306.

Hawthorne, F.C. (1997) Short-range order in amphiboles: a bond-valence approach. *Canadian Mineralogist* **35**, 203–218.

Hawthorne, F.C. & Della Ventura, G. (2007) Short-range order in amphiboles. *Reviews in Mineralogy and Geochemistry* **67**, 173–222.

Hawthorne, F.C. & Oberti, R. (2007) Amphiboles: Crystal chemistry. *Reviews in Mineralogy and Geochemistry* **67**, 1–54.

Hawthorne, F.C., Ungaretti, L., & Oberti, R. (1995) Site populations in minerals: terminology and presentation of results of crystal-structure refinement. *Canadian Mineralogist* **33**, 907–911.

Hawthorne, F.C., Oberti, R., & Sardone, N. (1996) Sodium at the *A* site in clinoamphiboles: the effects of composition on patterns of order. *Canadian Mineralogist* **34**, 577–593.

Hawthorne, F.C., Della Ventura, G., Oberti, R., Robert, J-L., & Iezzi, G. (2005) Short-range order in minerals: amphiboles. *Canadian Mineralogist* **43**, 1895–1920.

Hawthorne, F.C., Oberti, R., & Martin, R.F. (2006) Short-range order in amphiboles from the Bear Lake Diggings, Ontario. *Canadian Mineralogist* **44**, 1171–1179.

Karup-Møller, S. & Petersen, O.V. (1984) Tuperssuatsiaite, a new mineral species from the Ilı´maussaq intrusion in South Greenland. *Neues Jahrbuch für Mineralogie (Monatshefte)* **1984**, 501–512.

Perrault, G., Harvey, Y., & Pertsowsky, R. (1975) La yofortierite, un nouveau silicate hydrate de manganese de St.-Hilaire, P.Q. *Canadian Mineralogist* **13**, 68–74.

Pluth, J.J., Smith, J.V., Pushcharovsky, D.Y., Semenov, E.I., Bram, A., Riekel, C., Weber, H.P., & Broach, R.W. (1997) Third-generation synchrotron x-ray diffraction of 6-mm crystal of raite, approximate to $Na_3Mn_3Ti_{0.25}Si_8O_{20}(OH)_2{\cdot}10H_2O$, opens up new chemistry and physics of low- temperature minerals. *Proceedings of the National Academy of Sciences of the United States of America* **94**, 12263–12267.

Post, J.E. & Heaney, P.J. (2008) Synchrotron powder X-ray diffraction study of the structure and dehydration behavior of palygorskite. *American Mineralogist* **93**, 667–675.

Rancourt, D.G. & Ping, J.Y. (1991) Voigt-based methods for arbitrary-shape static hyperfine parameter distributions in Mössbauer spectroscopy. *Nuclear Instruments and Methods in Physics Research* **B58**, 85–97.

Shannon, R.D. (1976) Revised effective ionic radii and systematic studies of interatomic distances in halides and chalcogenides. *Acta Crystallographica* **A32**, 751–767.

Sheldrick, G.M. (2008) A short history of SHELX. *Acta Crystallographica* **A64**, 112–122.

von Knorring, O., Petersen, O.V., Karup-Møller, S., Leonardsen, E.S., & Condliffe, E. (1992) Tuperssuatsiaite from the Aris phonolite, Windhoek, Namibia. *Neues Jahrbuch für Mineralogie (Monatshefte)* **1992**, 145–152.

Yamnova, N.A., Egorov-Tismenko, Yu.K., & Khomyakov, A.P. (1996) Crystal structure of a new natural (Na,Mn,Ti)-phyllosilicate. *Crystallography Reviews* **42**, 239–244.

Received February 1, 2012, revised manuscript accepted March 27, 2013.